IJFAC

Indonesian Journal of Fundamental and Applied Chemistry

Article http://ijfac.unsri.ac.id

Study of Adsorption Isotherm and Thermodynamic Aspects of Congo Red and Procion Red over Natural and Zn/Fe Pillared Bentonite

Desnelli Desnelli[1,2,*], Heni Yohandini[1,2], Elisa Nurnawaty[1,3], and Poedji Loekitowati Hariani[1,2]

[1] Department of Chemistry, Faculty of Mathematics and Natural Science, Sriwjaya University, Jalan Palembang Prabumulih Km 32 Indralaya, Indonesia, 30662
[2] Research Centre of Advance Material and Nanocomposite, Faculty of Sciences and Mathematics, Universitas Sriwjaya, Jalan Palembang Prabumulih Km 32 Indralaya, Indonesia, 30662
[3] Department of Biology, Faculty of Mathematics and Natural Science, Sriwjaya University, Jalan Palembang Prabumulih Km 32 Indralaya, Indonesia, 30662

[*]*Corresponding Author: desnelli@unsri.ac.id*

Abstract

The effect of initial Congo Red and Procion Red concentration on isotherm adsorption and thermodynamic adsorption study using natural and Zn/Fe Pillared bentonite have been conducted. The adsorbents were also characterized by Fourier transform infrared (FTIR), X-Ray Diffraction (XRD), and Scanning electron microscope-energy dispersive X-Ray analysis (SEM-EDX). The study showed that the optimum dye removal of Congo Red and Procion Red was obtained at the initial dye concentration of 80 mg/L. The adsorption isotherm study showed that the Congo Red and Procion Red adsorption on natural and Zn/Fe Pillared bentonite followed the Freundlich isotherm model. The adsorption thermodynamics study showed that the adsorption of Congo Red and Procion Red occurred endothermically, whereas the positive value of entropy indicated a high level of disorder of adsorption for both dyes. Furthermore, the FTIR, XRD, and SEM-EDX analysis showed that the pillarization of Zn/Fe on bentonite successfully well occurred, and it could be concluded that the adsorption of Congo Red using natural and Zn/Fe pillared bentonite showed a better adsorption process than Procion Red.

Keywords: Bentonite, Pillared bentonite; Adsorption isotherm, Adsorption thermodynamic

Article Info

Received 8 May 2022
Received in revised 25 May 2022
Accepted 26 May 2022
Available online 25 June 2022

INTRODUCTION

The textile industry is vital in expanding the non-oil and gas economic sector in many developing countries. However, besides its significant role, the textile industry also poses quite severe problems for the environment, especially the disposal of liquid waste dyes [1]. Congo Red and Procion Red dyes are commonly found in the textile industry, and these dyes have an azo group (-N=N-), which have been reported to be carcinogenic, mutagenic, and teratogenic, and potentially damaging to the environment and organisms [2]. The high risk of this harmful dye to humans and the environment has led researchers to develop various methods to treat dye's waste.

Chemical, physical, and biological methods, including adsorption, biosorption, flocculation coagulation, ozonation, advanced oxidation, and membrane filtration, have been widely used to treat the waste of dyes [3]. Among the various dye removal methods, adsorption is the preferred and primary method due to its simplicity of design, low cost, ease of operation, and high efficiency [4]. Bentonite is one of the alternative adsorbents that is often used for dye adsorption because it is relatively cheap, non-toxic, and has a large specific surface area which can increase the adsorption capacity [5]. The adsorption capacity of bentonite is generally higher for cationic dyes than for anionic dyes due to the negative charge on the bentonite surface. Therefore, bentonite must be modified to increase its adsorption capacity against acidic dyes [6].

Modification of bentonite through pillarization has been widely carried out to increase its adsorption ability and dye removal [7]. Pillared bentonite can be synthesized by exchangeable cations into bentonite layers using single or mixed oligomeric polycations

such as Fe, Cr, Al, Co, Cu, Zr, Al/Cu, Al/Fe, and Al/Si. Cation exchange can lead to a tremendous increase in bentonite basal spacing [8]. The metal oxides Zn and Fe have been reported to have good abilities to azo dyes adsorption, respectively [9-10]. These metal oxides are also reported to have favorable physicochemical characteristics as adsorbents [11]. Based on that idea, Zn/Fe Pillared bentonite hypothetically has a great adsorption ability as well as dye removal than Natural bentonite.

The previous report has studied the effect of adsorbent weight, adsorption time, pH, and pseudo kinetic of adsorption Congo Red and Procion Red using Zn/Fe Pillared bentonite [12]. Further studies are needed to obtain more optimal adsorption results. Hence, this research would be focused on isotherm and thermodynamic studies of the adsorption of Congo Red and Procion Red using Zn/Fe Pillared bentonite, considering those parameters have not been reported yet. The adsorbent would also be characterized using Fourier Transform Infrared (FTIR) and Scanning Electron Microscope-Energy Dispersive X-ray (SEM-EDX) as well as compared with natural bentonite.

MATERIALS AND METHODS

Materials

Bentonite clay was provided from bentonite deposit placed in Lampung Province, Indonesia. All chemicals i.e zinc chloride ($ZnCl_2$, 98.0-100.5% purity), ferrous chloride ($FeCl_2$, ≥ 98.0% purity), Congo Red ($C_{32}H_{22}N_6Na_2O_6S_2$) (dye content of ≥75%), and Procion Red ($C_{19}H_{10}Cl_2N_6Na_2O_7S_2$) (dye content of 40%) were analytical grade purchased from Merck Millipore.

Synthesis of Zn/Fe Pillared Bentonite

Firstly, the bentonite was washed with distilled water and dried at 110 ˚C for one day. Zn/Fe Pillared bentonite was synthesized by preparing 12 g of 200-mesh bentonite dissolved in 120 mL of distilled water and stirred for 2 hours. The suspension was then pillared using a Zn/Fe solution by stirring for 24 hours. The solution was filtered, and the residue was dried using an oven at 100 ˚C and calcined using a muffle furnace for 2 hours at 400 ˚C. The product was characterized by XRD (Rigaku Minu Flex 600), FTIR (Shimadzu), and SEM-EDX (JEOL-JSM 6510 LA).

Adsorption Studies

Adsorption isotherm and thermodynamic aspects were conducted by varying the concentration of dye (20, 50, 80, 100, and 130 mg/L) and adsorption temperature (30, 50, 70 ˚C) with a 0.05 g of adsorbent, which dissolved in 50 mL of dye. The solution was shaken for 1 hour. The solution was then filtered, and the concentration of the remaining dye after the adsorption was measured using a using UV-Vis Spectrophotometer (Shimadzu) at λ max of 498 nm and 537 nm for Congo Red and Procion Red, respectively. The dye removal was calculated according to the difference in the initial and the final concentrations of the dye divided by the initial dye concentration as well. The adsorption isotherms were evaluated using the Langmuir and Freundlich model.

RESULTS AND DISCUSSION

Adsorbent Characterizations

Natural bentonite and Zn/Fe Pillared bentonite were characterized using FTIR, XRD, and SEM-EDX. The infrared spectra of Natural bentonite and Zn/Fe Pillared bentonite are shown in **Figure 1**. The infrared spectra of Natural bentonite and Zn/Fe Pillared bentonite. The spectra of Natural bentonite reveals a peak at 3636 cm^{-1}, indicating the presence of –OH groups segregated from the interlayer of bentonite by Si-OH and Al-OH silanols [6, 8]. The broadband at 3474 cm^{-1} was associated with adjacent silanol groups, and it could be observed that the absorption band tends to weaken after pillarization due to the calcination effect of Si-O-Si bond formation [13].

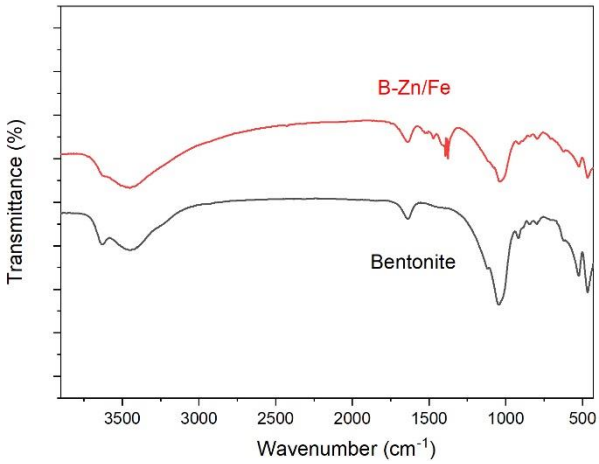

Figure 1. FTIR spectra of bentonite and Zn/Fe pillared bentonite

In the low-frequency region, the strong band at 1050 cm^{-1} indicates Si-O stretching vibrations in the bentonite plane, the peak at 916 cm^{-1} was associated with Al-OH-Al, the adsorption band in 620 cm^{-1} represents vibrations in the Al-O and Si-O planes [14, 15]. Furthermore, the low peaks at 674 cm^{-1} and 710 cm^{-1} indicate stretching vibrations of Fe-O. Fe-O bands are also found in Natural bentonite from dioctahedral or trioctahedral smectite [8]. The Zn-O stretching absorption is generally in the range of 400-700 cm^{-1}, in

this case, absorption at 525 cm^{-1} was presumably from Zn-O stretching vibration [10, 16].

The diffractogram of Natural bentonite and Zn/Fe Pillared bentonite are shown in **Figure 2**. The characteristic peaks at 2θ of 20.82˚, 28.81˚, 35.12˚, 61.92˚ indicated the montmorillonite structure. This pattern was in accordance with the standard JCPDS file (card no. 01-088-0831); this finding was consistent with similar a report [17]. From the diffractogram, it could be observed that there was an increase in basal spacing (d_{001}) from 11.21 to 15.65 nm. This increase was caused by the intercalation of hydrolyzed Zn/Fe in the bentonite interlayer through the formation of pillars. The inclusion of transition metals into the bentonite layer makes the reflection position of 001 can shift the angle by 2θ compared to bentonite [8].

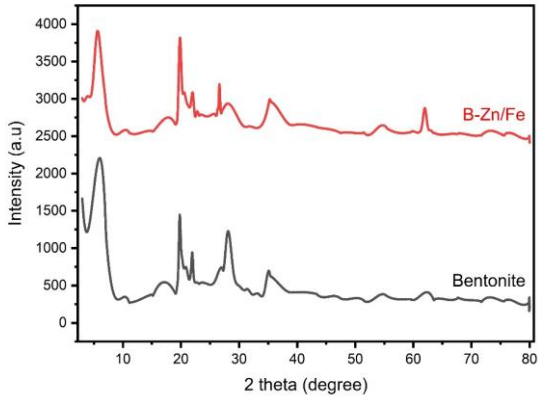

Figure 2. Diffractograms of Natural bentonite and Zn/Fe Pillared bentonite

Figure 2 shows that the 6˚ angle in the bentonite diffractogram shifts to a lower angle of 5.64˚, indicating that the intercalation in clay minerals has occurred [18]. The appearance of a new peak after pillarization at 2θ of 26.64˚ and 54.11˚ may indicated the presence of Zn/Fe metal oxide [19, 20], The peak was relatively difficult to observe and distinguish, presumably due to the low crystallinity as well as the concentration of metal oxide [21].

The SEM images of bentonite and Zn/Fe pillared bentonite are shown in **Figure 3**. It can be seen that Natural bentonite has a thin structure with sharp and irregular edges. The presence of Zn/Fe alters the lammeral structure of Natural bentonite and causes the formation of scattered granules from the Bentonite surface [8, 18]. This finding was consistent with Ain et al. [22] in the study bentonite pillarization using iron oxide. The morphological changes due to the pillarization of bentonite have also been reported by Satwikanitya et al. [23] using cobalt oxide. Furthmore, EDX analysis showed that the Zn content increased from 0 to 1.92 % and Fe from 0.68 to 0.89 %, respectively, which indicates that the Zn/Fe pillarization process well occurred.

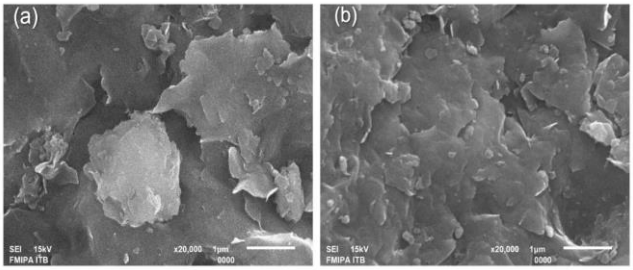

Figure 3. Morphological surface of (a) natural bentonite and (b) Zn/Fe pillared bentonite

Effect of Dye Initial Concentration

The efficiency of Congo Red and Procion Red removal by bentonite and B-Zn/Fe is shown in **Figure 4**. It can be seen that the percentage of dye removal increased with increasing dye concentration. After achieving an optimum dyes removal at 80 mg/L, surprisingly, the percentage of dye removal was gradually decreased. A similar trend has been reported by Al-Ghouti et al. [24] in the study of adsorption of methylene blue using cellulosic olive stones biomass.

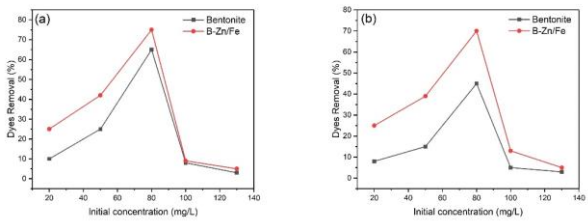

Figure 4. Effect of initial concentration on dyes removal of (a) Congo Red and (b) Porcion red

According to Albroomi et al. [25], at low dye concentrations, the availability of empty pores and the active site on the adsorbent was high. However, the fractional adsorption of dyes and mass transfer decreases, leading to a lower percentage of dye removal. As the dye concentration increases, the mass transfer of the dye also increases, and more bonds are available, leading to an increase in the percentage of dye removal [26]. Furthermore, the ratio of dye molecules to available binding sites did not support mass transfer at higher concentrations. In addition, at high dye concentrations, the mass transfer of dye molecules is higher due to an increase in the ratio of the dye to the binding site. Nevertheless, the number of binding sites available on the adsorbent will decrease and disappear when the dye molecules occupy these

sites [27]. This was what caused at high dye concentrations, which more than 80 mg/L, the percentage of dye removal decreased. **Figure 4** also shows that the dye removal of the pillared Zn/Fe was more significant than Natural bentonite. This condition certainly showed that the pillarization using Zn/Fe oxide could be associated with an increase in the ability of bentonite as an adsorbent [28]; This was due to the availability of Zn/Fe active sites on the bentonite surface, as a result the percentage of dye removal becomes much more effective [29].

Adsorption Isotherm Study

The Langmuir and Freundlich isotherm data can be seen in **Table 1** and **Table 2** for Congo Red and Procion Red, respectively. According to the Langmuir Isotherm model, it can be seen that increasing the temperature will increase the adsorption of both dyes over the adsorbent; this indicated that the adsorption was favorable at a higher temperature [30]. The higher adsorption capacity for Zn/Fe Pillared bentonite corresponded to the Zn/Fe intercalation in bentonite. According to Aziz et al. [31] increasing the distance between layers via intercalation would facilitate dye adsorption onto Zn/Fe Pillared bentonite. Furthermore, the K_L value between 0 and 1 indicated that Zn/Fe Pillared bentonite was a suitable adsorbent for the adsorption of both dyes [32]. Meanwhile, it was also found in the Freundlich model that the K_F value increased with increasing adsorption temperature, which could be explained by the increase in the rate of dye diffusion into the pores. Thus, a high adsorption ability to the surface of the adsorbent was obtained due to the high-temperature adsorption [33].

Table 1. The adsorption isotherm data using the Freundlich and Langmuir model on Natural bentonite and Zn/Fe Pillared bentonite on Congo Red adsorption

Temperature (˚C)	Freundlich model			Langmuir model		
	Parameter	Natural Bentonite	Zn/Fe Pillared Bentonite	Parameter	Natural Bentonite	Zn/Fe Pillared Bentonite
30	K_F	0.8406	0.7698	K_L	0.0210	0.0601
	n	2.1123	0.4357	Q_m	6.1425	12.1359
	R^2	0.9294	0.9504	R^2	0.2563	0.6532
50	K_F	0.8695	0.9016	K_L	0.0061	0.0368
	n	1.2397	0.6957	Q_m	46.0829	52.0833
	R^2	0.8676	0.9059	R^2	0.076	0.439
70	K_F	1.0143	1.1763	K_L	0.0021	0.0157
	n	0.9698	1.0937	Q_m	298.7	555.5
	R^2	0.9498	0.7327	R^2	0.0274	0.0643

Table 2. The adsorption isotherm data using the Freundlich and Langmuir model on Natural bentonite and Zn/Fe Pillared bentonite in Procion Red adsorption

Temperature (˚C)	Freundlich model			Langmuir model		
	Parameter	Natural Bentonite	Zn/Fe Pillared Bentonite	Parameter	Natural Bentonite	Zn/Fe Pillared Bentonite
30	K_F	0.08007	0.9641	K_L	0.0311	0.1792
	n	2.3320	0.9493	Q_m	4.9480	67.5334
	R^2	0.3724	0.9417	R^2	0.1002	0.1365
50	K_F	0.1078	0.9430	K_L	0.0219	0.0227
	n	1.1659	1.0474	Q_m	17.2063	83.6435
	R^2	0.8501	0.9845	R^2	0.1574	0.998
70	K_F	1.0998	2.2420	K_L	0.0043	0.0186
	n	1.8749	0.7727	Q_m	10.8886	83.4127
	R^2	0.7518	0.8547	R^2	0.02559	0.7844

According to the adsorption isotherm study, the correlation coefficient (R^2) Freundlich models have higher values than the Langmuir model. This condition indicates that the adsorption of Congo Red and Procion Red dye adsorbents using natural and Pillared bentonite was more suitable using the Freundlich adsorption isotherm model and indicates that the adsorption occurs in a multilayer system rather than a monolayer with a heterogeneous adsorbent surface [34-36].

Adsorption Thermodynamics Aspect

The thermodynamic adsorption parameters using natural and Zn/Fe Pillared bentonite were presented in **Table 3** for Congo Red and **Table 4** for Procion Red, respectively. It can be seen that the enthalpy value of Congo Red and Procion Red were positive; this indicated the adsorption endothermically occurred [24]. In addition, the positive entropy of each dye indicated the randomness between the solid-liquid phase during the absorption process [37]. This condition indicates surface changes due to the interaction of the dye molecules with the active site of the adsorbent. According to Nasuha and Hameed [38], the randomness in the system was also caused by dye ions which replaced the water adsorbed prior on the surface of the adsorbent.

Table 3. The Adsorption energy (E), Entropy (ΔS) and Enthalpy (ΔH) on Congo Red adsorption using Natural bentonite and Pillared bentonite adsorbent

Concentration (mg/L)	ΔS (J/mol)		ΔH (kJ/mol)		E (kJ/mol)
	Natural bentonite	Zn/Fe Pillared Bentonite	Natural bentonite	Zn/Fe Pillared Bentonite	
20	66.9	84.78	24.60	48.94	46.212
50	46.27	86.36	17.84	43.28	32.787
80	30.26	78.87	13.32	35.44	23.087
100	25.81	62.93	11.93	28.15	20.275
130	22.22	52.85	12.58	24.22	17.375

Table 4. The Adsorption Energy (E), entropy (ΔS) and Enthalpy (ΔH) on Procion Red adsorption using Natural bentonite and Zn/Fe Pillared bentonite adsorbent

Concentration (mg/L)	ΔS (J/mol)		ΔH (kJ/mol)		E (kJ/mol)
	Natural bentonite	Zn/Fe Pillared Bentonite	Natural bentonite	Zn/Fe Pillared Bentonite	
20	39.87	96.55	15.83	28.43	4.588
50	36.71	77.48	9.88	21.39	4.347
80	22.12	56.03	5.15	15.58	2. 328
100	13.80	37.11	2.43	9.73	2.732
130	10.55	25.09	3.19	3.86	1.576

CONCLUSION

This research studied the adsorption isotherm and thermodynamics of adsorption of Congo Red and Procion Red on Zn/Fe Pillared bentonite. The FTIR, XRD, and SEM-EDX analysis showed that the Zn/Fe pillarization of bentonite was successful. Adsorption studies showed that the optimum condition for dye removal was achieved at the initial dye concentration of 80 mg/L. The Congo Red and Procion Red adsorption using bentonite and Pillared bentonite were more suitable using the Freundlich model, which takes place in multilayers system with heterogeneous adsorbent surfaces. Thermodynamic studies showed that Congo Red and Procion Red adsorption tends to occur endothermic with a positive entropy value of both adsorbents. Overall, the pillarization of bentonite using Zn/Fe metal oxide of bentonite could increase with favorable adsorption onto Congo Red and Procion Red.

REFERENCES

[1] Rahman, T. Urabe, and N. Kishimoto, "Color removal of reactive procion dyes by clay adsorbents," *Procedia Environ. Sci.*, vol. 17, pp. 270–278, 2013, doi: 10.1016/j.proenv.2013.02.038.

[2] J. Georgin, B. D. S. Marques, J. D. S. Salla, E. L. Foletto, D. Allasia, and G. L. Dotto, "Removal of procion red dye from colored effluents using H_2SO_4-/HNO_3-treated avocado shells (Persea americana) as adsorbent," *Environ. Sci. Pollut. Res.*, vol. 25, no. 7, pp. 6429–6442, 2018, doi: 10.1007/s11356-017-0975-1.

[3] J. O. Amode, J. H. Santos, Z. Md. Alam, A. H. Mirza, and C. C. Mei, "Adsorption of methylene blue from aqueous solution using untreated and treated (Metroxylon spp.) waste adsorbent: equilibrium and kinetics studies," *Int. J. Ind.*

Chem., vol. 7, no. 3, pp. 333–345, 2016, doi: 10.1007/s40090-016-0085-9.

[4] S. Jayanthi, N. Krishnarao Eswar, S. A. Singh, K. Chatterjee, G. Madras, and A. K. Sood, "Macroporous three-dimensional graphene oxide foams for dye adsorption and antibacterial applications," *RSC Adv.*, vol. 6, no. 2, pp. 1231–1242, 2016, doi: 10.1039/c5ra19925e.

[5] F. Ayari, G. Manai, S. Khelifi, and M. Trabelsi-Ayadi, "Treatment of anionic dye aqueous solution using Ti, HDTMA and Al/Fe pillared bentonite. Essay to regenerate the adsorbent," *J. Saudi Chem. Soc.*, vol. 23, no. 3, pp. 294–306, 2019, doi: 10.1016/j.jscs.2018.08.001.

[6] E. Fosso-Kankeu, F. Waanders, and C. L. Fourie, "Adsorption of congo red by surfactant-impregnated bentonite clay," *Desalin. Water Treat.*, vol. 57, no. 57, pp. 27663–27671, 2016, doi: 10.1080/19443994.2016.1177599.

[7] S. Khelifi, F. Ayari, A. Choukchou-Braham, and D. Ben Hassan Chehimi, "The remarkable effect of Al–Fe pillaring on the adsorption and catalytic activity of natural Tunisian bentonite in the degradation of azo dye," *J. Porous Mater.*, vol. 25, no. 3, pp. 885–896, 2018, doi: 10.1007/s10934-017-0500-4.

[8] A. Kadeche, A. Ramdani, M. Adjdir, A. Guendouzi, S. Taleb, M. Kaid, and A. Derantani, "Preparation, characterization and application of Fe-pillared bentonite to the removal of Coomassie blue dye from aqueous solutions," *Res. Chem. Intermed.*, vol. 46, no. 11, pp. 4985–5008, 2020, doi: 10.1007/s11164-020-04236-2.

[9] M. N. Zafar, Q. Dar, F. Nawaz, M. N. Zafar, M. Iqbal, and M. F. Nazar, "Effective adsorptive removal of azo dyes over spherical ZnO nanoparticles," *J. Mater. Res. Technol.*, vol. 8, no. 1, pp. 713–725, 2019, doi: 10.1016/j.jmrt.2018.06.002.

[10] P. K. Ngoc, T. K. Mac, H. T. Nguyen, D. T. Viet, T. D. Thanh, P. V. Vinh, B. T. Phan, A. T. Duong, and R. Das, "Excellent organic dye adsorption capacity and recyclability of hydrothermally synthesized α-Fe_2O_3 nanoplates and nanorices," *J. Sci. Adv. Mater. Devices*, vol. 6, no. 2, pp. 245–253, 2021, doi: 10.1016/j.jsamd.2021.02.006.

[11] S. I. Siddiqui and S. A. Chaudhry, "Iron oxide and its modified forms as an adsorbent for arsenic removal: A comprehensive recent advancement," *Process Saf. Environ. Prot.*, vol. 111, pp. 592–626, 2017, doi: 10.1016/j.psep.2017.08.009.

[12] D. Desnelli, W. R. Asri, Hasanudin, M. Said, and P. L. Hariani, "Removal of congo red and procion red using Zn/Fe pillared bentonite," *IOP Conf. Series: Earth and Environmental Science*, 2021, vol. 926, p. 012051, doi: 10.1088/1755-1315/926/1/012051.

[13] L. G. Yan, L. L. Qin, H. Q. Yu, S. Li, R. R. Shan, and B. Du, "Adsorption of acid dyes from aqueous solution by CTMAB modified bentonite: Kinetic and isotherm modeling," *J. Mol. Liq.*, vol. 211, pp. 1074–1081, 2015, doi: 10.1016/j.molliq.2015.08.032.

[14] M. Toor, B. Jin, S. Dai, and V. Vimonses, "Activating natural bentonite as a cost-effective adsorbent for removal of Congo-red in wastewater," *J. Ind. Eng. Chem.*, vol. 21, pp. 653–661, 2015, doi: 10.1016/j.jiec.2014.03.033.

[15] B. B. Pajarito, K. C. Castañeda, S. D. M. Jeresano, and D. A. N. Repoquit, "Reduction of offensive odor from natural rubber using zinc-modified bentonite," *Adv. Mater. Sci. Eng.*, vol. 2018, 2018, doi: 10.1155/2018/9102825.

[16] M. Sangeeta, K. V. Karthik, R. Ravishankar, K. S. Anantharaju, H. Nagabhushana, K. Jeetendra, Y. S. Vidya and L. Renuka, "Synthesis of ZnO, MgO and ZnO/MgO by Solution Combustion Method: Characterization and Photocatalytic Studies," *Mater. Today Proc.*, vol. 4, no. 11, pp. 11791–11798, 2017, doi: 10.1016/j.matpr.2017.09.096.

[17] R. S. Hebbar, A. M. Isloor, B. Prabhu, Inamuddin, A. M. Asiri, and A. F. Ismail, "Removal of metal ions and humic acids through polyetherimide membrane with grafted bentonite clay," *Sci. Rep.*, vol. 8, no. 1, pp. 1–17, 2018.

[18] Z. Huang, Y. Li, W. Chen, J. Shi, N. Zhang, X. Wang, Z. Li, L. Gao and Y. Zhang, "Modified bentonite adsorption of organic pollutants of dye wastewater," *Mater. Chem. Phys.*, vol. 202, pp. 266–276, 2017.

[19] S. Lubis, Sheilatina, and Murisna, "Synthesis, characterization and photocatalytic activity of α-Fe_2O_3/bentonite composite prepared by mechanical milling," *J. Phys. Conf. Ser.*, vol. 1116, no. 4, 2018.

[20] S. Mustapha, J. O. Tijani, M. M. Ndamitso, S. A. Abdulkareem, D. T. Shuaib, A. K. Mohammed and A. Sumaila, "The role of kaolin and kaolin/ZnO nanoadsorbents in adsorption studies for tannery wastewater treatment," *Sci.*

Rep., vol. 10, no. 1, pp. 1–22, 2020, doi: 10.1038/s41598-020-69808-z.

[21] J. Siregar, K. Sebayang, B. Yuliarto, and S. Humaidi, "XRD characterization of Fe_3O_4-ZnO nanocomposite material by the hydrothermal method," *AIP Conf. Proc.*, vol. 2221, no. 1, p. 110008, 2020, doi: 10.1063/5.0003210.

[22] Q. U. Ain, U. Rasheed, M. Yaseen, H. Zhang, and Z. Tong, "Superior dye degradation and adsorption capability of polydopamine modified Fe_3O_4-pillared bentonite composite," *J. Hazard. Mater.*, vol. 397, p. 122758, 2020, doi: 10.1016/j.jhazmat.2020.122758.

[23] P. Satwikanitya, I. Prasetyo, M. Fahrurrozi, and T. Ariyanto, "Adsorption of ethylene using cobalt oxide-loaded pillared clay," *J. Eng. Technol. Sci.*, vol. 52, no. 3, pp. 424–435, 2020, doi: 10.5614/j.eng.technol.sci.2020.52.3.9.

[24] M. A. Al-Ghouti and R. S. Al-Absi, "Mechanistic understanding of the adsorption and thermodynamic aspects of cationic methylene blue dye onto cellulosic olive stones biomass from wastewater," *Sci. Rep.*, vol. 10, no. 1, pp. 1–18, 2020, doi: 10.1038/s41598-020-72996-3.

[25] H. I. Albroomi, M. A. Elsayed, A. Baraka, and M. A. Abdelmaged, "Batch and fixed-bed adsorption of tartrazine azo-dye onto activated carbon prepared from apricot stones," *Appl. Water Sci.*, vol. 7, no. 4, pp. 2063–2074, 2017.

[26] S. Radoor, J. Karayil, J. Parameswaranpillai, and S. Siengchin, "removal of anionic dye congo red from aqueous environment using polyvinyl alcohol/sodium alginate/ZSM-5 zeolite membrane," *Sci. Rep.*, vol. 10, no. 1, pp. 1–15, 2020.

[27] I. J. Idan, L. C. Abdullah, T. S. Y. Choong, and S. N. A. B. M. Jamil, "Equilibrium, kinetics and thermodynamic adsorption studies of acid dyes on adsorbent developed from kenaf core fiber," *Adsorpt. Sci. Technol.*, vol. 36, no. 1–2, pp. 694–712, 2018.

[28] W. Huang, J. Chen, F. He, J. Tang, D. Li and Y. Zhu, "Effective phosphate adsorption by Zr/Al-pillared montmorillonite: Insight into equilibrium, kinetics and thermodynamics," *Appl. Clay Sci.*, vol. 104, pp. 252–260, 2015.

[29] O. Issaoui, H. Ben Amor, M. Ismail, and M. R. Jeday, "Preparation of Al-pillared clay and application of methylene blue adsorption," *Int. Conf. Green Energy Convers. Syst. 2017*, pp. 1–4, 2017.

[30] R. Huang, L. Zhang, P. Hu, and J. Wang, "Adsorptive removal of congo red from aqueous solutions using crosslinked chitosan and crosslinked chitosan immobilized bentonite," *Int. J. Biol. Macromol.*, vol. 86, pp. 496–504, 2016, doi: 10.1016/j.ijbiomac.2016.01.083.

[31] B. K. Aziz, D. M. Salh, S. Kaufhold, and P. Bertier, "The high efficiency of anionic dye removal using Ce-Al13/pillared clay from Darbandikhan natural clay," *Molecules*, vol. 24, no. 15, pp. 1–15, 2019, doi: 10.3390/molecules24152720.

[32] M. Stjepanović, N. Velić, A. Galić, I. Kosović, T. Jakovljević, and M. Habuda-Stanić, "From waste to biosorbent: Removal of congo red from water by waste wood biomass," *Water*, vol. 13, no. 3, 2021.

[33] N. S. Sulaiman, M. H. Mohamad Amini, M. Danish, O. Sulaiman, and R. Hashim, "Kinetics, thermodynamics, and isotherms of methylene blue adsorption study onto cassava stem activated carbon," *Water*, vol. 13, no. 20. 2021.

[34] C. Phawachalotorn and N. Suwanpayak, "The efficiency of mangosteen peel for dye removal," *J. Phys. Conf. Ser.*, vol. 1719, no. 1, 2021.

[35] V. S. Munagapati, V. Yarramuthi, Y. Kim, K. M. Lee, and D. S. Kim, "Removal of anionic dyes (reactive black 5 and congo red) from aqueous solutions using banana peel powder as an adsorbent," *Ecotoxicol. Environ. Saf.*, vol. 148, pp. 601–607, 2018.

[36] T. H. Nazifa, N. Habba, Salmiati, A. Aris, and T. Hadibarata, "Adsorption of procion red MX-5B and crystal violet dyes from aqueous solution onto corncob activated carbon," *J. Chinese Chem. Soc.*, vol. 65, no. 2, pp. 259–270, 2018, doi: 10.1002/jccs.201700242.

[37] C. Djelloul, A. Hasseine, and O. Hamdaoui, "Adsorption of cationic dye from aqueous solution by milk thistle seeds: Isotherm, kinetic and thermodynamic studies," *Desalin. Water Treat.*, vol. 78, pp. 313–320, 2017, doi: 10.5004/dwt.2017.20920.

[38] N. Nasuha and B. H. Hameed, "Adsorption of methylene blue from aqueous solution onto NaOH modified rejected tea," *Chem. Eng. J.*, vol. 166, no. 2, pp. 783–786, 2011, doi: 10.1016/J.CEJ.2010.11.012.